

**ESTIMATION OF WINTER WHEAT CROP GROWTH  
PARAMETERS USING SENTINEL-1A SAR DATA****5.1 INTRODUCTION**

In agriculture, crop growth monitoring and yield estimation are of common purpose. Useful and an attractive approach is the remote sensing for the monitoring of agricultural crop growth parameters (Beriaux et al., 2013). The crop parameters are one of the most useful indicators for the vegetation development, monitoring of crop growth and yield prediction. The economic growth of several countries depends on the production of wheat crop. Due to its importance, it is needed to estimate the full crop growth by obtaining the precise and well-timed information about the condition of a crop. Since 1970s, several ground based instruments have shown significant sensitivity of radar for the estimation of crop growth parameters (Ulaby et al., 1986; Prasad, 2011; Kim et al., 2014). SAR signals with the crop growth parameters have been reported for the wheat (Cookmartin et al., 2000; McNairn et al., 2002; Mattia et al., 2003), rice (Chakraborty et al., 2005; Inoue and Sakaiya, 2013; Gupta et al., 2015b), soil moisture and grass land (Baghdadi et al., 2016), sunflower (Fieuzal and Baup, 2016), corn (Beriaux et al., 2013) and soybean (Betbeder et al., 2016). Indeed, SAR sensors offer a good temporal resolution throughout the crop growing season because the transmitted microwave energy is barely affected by the atmospheric conditions (Beriaux et al., 2013).

Several algorithms have been developed for the regression analysis to estimate the crop growth parameters from SAR and optical remotely sensed data. RFR is the emerging and precise prediction algorithm among the various machine learning

algorithms. This algorithm is relatively robust in regard to outliers and it can model complex interactions among input variables. RFR can run efficiently on large data-sets and can handle adequately thousands of input variables without variable deletion. Algorithm is not sensitive to noise or overfitting. The performance of RFR algorithm depends on determining the number of trees and predictors in each node to achieve better results (Shataee et al., 2012). The number of regression trees grown is based on the bootstrap sample of the observations and number of predictors at each node (Mutanga et al., 2012). Thus, the total 224 numbers of trees and 2 number of predictor variables are tested at each node. The RFR was found less sensitive with the validation data-set than the SVR algorithm for the estimation of wheat crop LAI (Siegmann and Jarmer, 2015). On changing the number of hidden layer nodes, the ANN performance showed extreme sensitivity to small network sizes and insensitivity to large network sizes (Kavzoglu and Mather, 2003). Robustness of RFR algorithm over SVR and ANNR has been shown for the estimation of wheat crop biomass (Wang et al., 2016). RFR algorithm was used mostly for the forest parameters estimation (Mutanga et al., 2012; Baghdadi et al., 2015). Only few studies have been reported for the regression analysis using RFR algorithm including estimation of agricultural crops parameters (Vuolo et al., 2013; Wang et al., 2016).

SVR algorithm is another algorithm that became as popular as RFR in the last few years in the field of geo-/ bio-physical parameters estimation. The SVR has provided the better results in comparison to RFR and partial least-squares regression for the prediction of wheat crop LAI using hyperspectral data (Siegmann and Jarmer, 2015). The SVR algorithm based retrieval of LAI provides a reasonably good agreement with the field derived LAI from multi-angle imaging spectroradiometer (Durbha et al., 2007). Their results obtained using SVR algorithm pointed out its good

intrinsic generalization ability and robustness to noise even with the limited reference samples. SVR was also found convenient for the biophysical parameters estimation of wheat, garlic, onion, corn, potato, sunflower, sugar beet, vineyard and alfalfa using CHRIS/ PROBA spaceborne sensor data (Tuia et al., 2011). The algorithm has shown great capability to predict plant biophysical parameters by relating spectral information to in-situ samples (Camps-Valls et al., 2006; Verrelst et al., 2012).

The effectiveness of ANNR algorithm has been tested on the space borne and test bed data-sets for the retrieval of crop parameters (Del Frate et al., 2004; Gupta et al., 2015a; 2016). Soil moisture and wheat crop growth variables retrieval using microwave radiometry were done by ANNR model (Del Frate et al., 2003). RF, SVR and k-NN were compared for the estimation of forest attributes (volume, basal area and tree number) using ASTER satellite data and utility of RF and SVM was shown over k-NN (Shataee et al., 2012). Another comparative study showed better performance of SVR when combination of LiDAR and Landsat TM data were used for the estimation of forest volume and basal area by RF, SVR, k-NN, ANN (Joibary, 2013). A review for the better understanding of the SVR and ANNR for the retrieval of biomass and soil moisture is given by Ali et al. (2015).

The recently launched Sentinel-1A as well as whole Copernicus program including Sentinel-2 optical data solved the problems regarding the cost of images internationally. Since ESA offers a free data distribution policy. Sentinel-1A satellite provides long term operational services in agriculture, environment, climate and security. The results of the present study show the significance of Sentinel-1A data for the accurate estimation of winter wheat crop growth parameters for effective crop growth monitoring. The present study is different from the latest SAR studies because very few studies were done using Sentinel-1A SAR data (Hornáček et al., 2012;

Navarro et al., 2016). The aim of the present study is to estimate and compare the winter wheat crop growth variables i.e. LAI, VWC, fresh biomass (FB), dry biomass (DB) and PH using Sentinel-1A SAR data at C-band by RFR, SVR, ANNR and LR algorithms.

## 5.2 WINTER WHEAT CROP GROWTH STAGES

In Indian context, the life cycle of winter wheat crop depends on the environmental conditions and the varieties of the crop. It is important to know the various growth stages of the winter wheat crop for the better understanding of the microwave response of crop growth variables. The five major growth stages of the winter wheat crop such as i.e. (a) tillering; (b) jointing; (c) booting; (d) heading; and (e) ripening are shown in Figure 5.1.

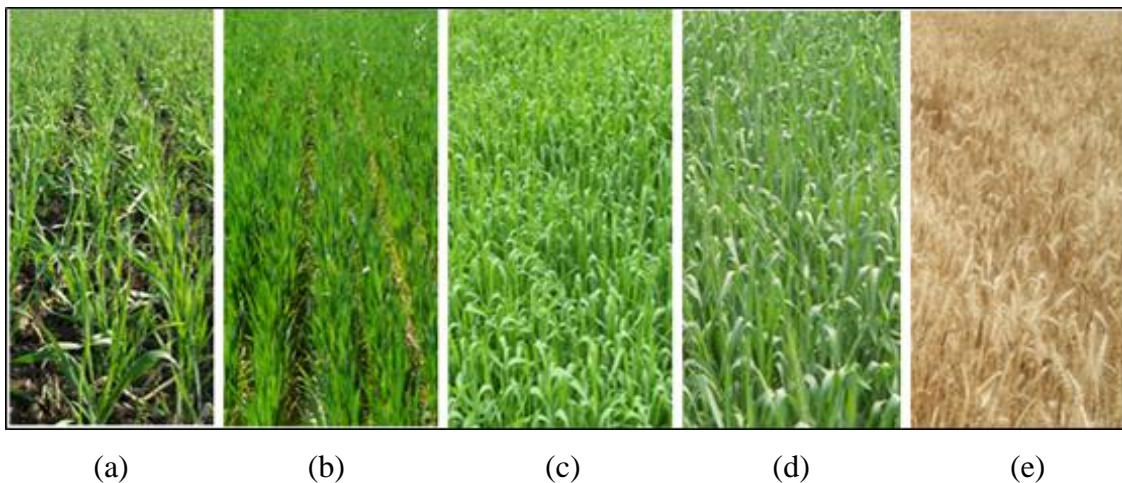


**Figure 5.1** Winter wheat crop growth stages: (a) tillering; (b) jointing; (c) booting; (d) heading; and (e) ripening

Unlike bare soil surfaces, it is difficult to predict backscattering of vegetated surfaces accurately because of several factors including plant biomass, structure (leaf size, LAI, stem/ plant density etc.); surface roughness, soil moisture as well as their interactions with the sensor configurations, such as polarization, frequency and incidence angle (Inoue et al., 2002; Graham and Harris, 2003). The backscattering of a vegetation canopy strongly depends on the angles of orientation of the scatterers (Gherboudj et al., 2011). As an example, the backscattering of wheat crop fields

decreases slowly on increasing the incidence angle because the leaves of wheat crop are mostly vertically oriented. For the pea crop fields, the backscattering decreases rapidly with increasing angle of incidence due to mostly horizontally oriented leaves of the pea crops (Karam and Fung, 1989). Several studies have shown significant correlation of the radar signal with the crop growth parameters, however the interpretation of backscattering coefficients for the crop monitoring is not always absolute (Briscoand Brown, 1998).

### **5.3 MATERIALS AND METHODOLOGY**

#### **5.3.1 Study area**

The study area is shown in Figure 5.2 using Sentinel-1A satellite image at VV polarization.



**Figure 5.2** The study area using Sentinel-1A satellite image at VV polarization

### **5.3.2 Measurements of winter wheat crop growth parameters**

Generally, wheat crop is grown in winter season in the North India. In-situ measurements of LAI, VWC, FB, DB and PH values were carried out from 8 January to 29 April 2015 in Varanasi district, India. The wheat crop field is characterized by an almost flat topography and average parcels. The maximum average height of winter wheat (PBW 343) crop was found 86.5 cm during entire observation. An instrument namely LAI-2200C (LI-COR Inc., USA) Plant Canopy Analyzer was used for the LAI measurements within the wheat field. The LAI is defined as the ratio of total upper leaf surface of the crop divided by the surface area of the ground on which crop is grown. Total 15 samples are collected at 3 different subplots of 1 m<sup>2</sup> area in the 95 m x 80 m wheat field for the LAI and PH measurements at every growth stage and satellite pass. The PH measurement was done manually using scale measurement at every growth stage. For the biomass measurements, the samples were collected in the subplots of 1 m<sup>2</sup> area in the crop field and sealed in the plastic bags. The FB samples were weighted using digital weighing scale before putting it in to the oven. The average FB per square meter was computed from the subplot measurements. After weighted FB, the samples were put in to the oven to make dry at 100 °C for the 24h. Samples were weighted again after getting dried in the oven to find the DB per square meter. The VWC of the plant is the total water content present in the plant constituents. The VWC per meter square area was calculated by subtracting DB from the FB samples. The average values of the LAI, VWC, FB, DB and PH samples were used for the analysis. Sampling was done very carefully to avoid the possibility of variability in the measurements of each winter wheat crop growth variable at each and every stage. The in-situ measurements were done at the same date of satellite data acquisition.

### 5.3.3 Satellite data collection and processing

Sentinel-1A SAR sensor carrying C-band having frequency 5.405 GHz was launched on 3 April 2014 by the ESA. Five different dates (8 January 2015 to 29 April 2015) satellite images at VV polarization were downloaded (<https://scihub.copernicus.eu/dhus/#/home>) for the full growth period of winter wheat crop grown in the Varanasi district. The characteristics of Ground Range Detected (GRD) Sentinel-1A data are described in the Table 5.1.

**Table 5.1** Sentinel-1A SAR satellite data specification

Satellite and band	Date of acquisition	Mode	Pass direction	Polarization	Product type	Resolution (m x m)	Product level
Sentinel-1A (SAR-C)	08/01/2015	IW	Ascending	VV	GRD	5x20	L1
	25/02/2015	IW	Ascending	VV	GRD	5x20	L1
	05/03/2015	IW	Descending	VV	GRD	5x20	L1
	21/03/2015	IW	Ascending	VV	GRD	5x20	L1
	29/04/2015	IW	Descending	VV	GRD	5x20	L1

The SNAP (Sentinels Application Platform) software version 1.1.1 particularly Sentinel-1 toolbox (S-1 TBX) freely downloaded (<http://step.esa.int/main/download/>) was used for the pre-processing of the SAR data-sets. Images were radiometrically calibrated and refined lee filter was used for the speckle filtering. Geometric correction was done by applying ellipsoid correction after speckle filtering of images. The radar cross section (sigma nought) was converted from natural values to dB backscatter coefficient.

### 5.3.4 Random forest regression algorithm

RFR is an ensemble algorithm that combines a large set of decision trees. Each tree is built using a deterministic algorithm by selecting a random set of variables and a random sample from the training data-set (Breiman, 2001). A decision tree represents a set of conditions that are applied from a root to a leaf of the tree and each tree is trained on a bootstrap sample of the original training data-set (Breiman et al., 1984). A decision tree is fitted to each of the bootstrap samples and to each node per tree. A small set of

input variables selected from the total set is randomly considered for binary partitioning (Rodriguez-Galiano et al., 2014). In the RFR, each tree was built with two-thirds of randomly selected (bootstrap samples) training data, whereas remaining one third (out-of-bag samples) data was used for model internal validation (Siegmann and Jarmer, 2015). The number of regression trees (ntree; 224) and the number of input variables per node (mtry; 2) were optimized using training data-set that provided the lowest root mean square errors (RMSE). The optimized number of trees and number of input variables per node were selected that could predict the winter wheat growth parameters accurately.

### **5.3.5 Support vector regression algorithm**

SVM algorithm has shown its robustness for the classification (Mishra et al., 2014). The algorithm was extended for the regression problems, i.e. usually called as SVR (Vapnik, 1995). SVR was used to estimate the linear dependency between pairs of n-dimensional input vectors and 1-dimensional target variables by fitting an optimal approximating hyperplane for a set of training samples (Monnet et al., 2011). SVR algorithm provides good generalization capabilities, robust to high input space dimension, fast, low number of samples and provides sparse solutions where only the most relevant samples of the training data are weighted resulting in low computational cost and memory requirements (Durbha et al., 2007). SVR algorithm depends on the proper setting of meta-parameters i.e. kernel function, loss function and error penalty factor  $C$ . The parameter  $C$  determines the trade off between the model complexity and the degree to which deviations larger than  $\varepsilon$  are tolerated in the optimization formulation. The parameter  $\varepsilon$  controls the width of the  $\varepsilon$ -insensitive zone. It is used to fit the training data and can affect the number of support vectors used to construct the regression function (Vapnik, 1995). The commonly used radial basis kernel function



(RBF) was applied for the SVR algorithm. The cross validation procedure is used to optimize these parameters including RBF kernel parameter  $\sigma$ ,  $\varepsilon$  and  $C$  yielding values 1, 1 and 8 respectively.

### **5.3.6 Artificial neural network regression algorithm**

The back propagation ANN algorithm is used to train the multilayer perceptron. The artificial neurons are organized in three different layers such as input, hidden and output layers (Kavzoglu and Mather, 2003). The ANN model is developed using input data-set ( $\sigma^\circ$ ) at input layer neurons and output data-sets (LAI, PH, FB, DB and VWC) at output layer neurons. The output values computed at input layer neurons are taken as the inputs of hidden layer neurons. The output values computed by the hidden layer neurons are taken as the input values for output layer neurons. The computed output values are compared with the target values. The computed error between output of ANN and target value is sent backwards to get the optimum accuracy by changing of weight and bias values. We optimized ANN with tan-sigmoid transfer function at hidden neurons and log-sigmoid transfer function at output neurons using the Levenberg–Marquardt algorithm. One neuron in the input layer, ten neurons in the hidden layer and one neuron in the output layer was used. Only one hidden layer was used to perform the ANN algorithm. The error-trial method was used to optimize the ANN parameters (Haykin, 1994).

### **5.3.7 Linear regression algorithm**

The linear regression (LR) algorithm modelled the data using linear predictors function and unknown parameters of the algorithm. These unknown parameters were determined using measured crop growth variables and computed backscattering coefficient at several growth stages of winter wheat crop. The algorithm establishes the

linear relationship by fitting linear equation between explanatory variable ( $x_i$ ) and dependent variable ( $y_i$ ). The LR algorithm can be represented by the Equation 4.1.

$$y_i = bx_i + a \quad (4.1)$$

Where  $i = 1, \dots, n$ ,  $a$  and  $b$  are the intercept and slope respectively. The coefficients (intercept and slope) were computed by the least square method.

### 5.3.8 Validation

The total number of sample data corresponding to different dates was interpolated in to 112 numbers of samples at the interval of one day. The performance of RFR, SVR, ANNR and LR algorithms was validated by splitting pooled data randomly into training data-set and testing data-set ( $2/3^{\text{rd}}$  and  $1/3^{\text{rd}}$  of the pooled data respectively). The training data-set was used for the optimization of RFR, SVR, ANNR and LR algorithms, whereas the testing data-set was used to examine the performance and reliability of the algorithms. In total, 73 samples were taken as the training data-sets and 39 samples were taken as the testing data-sets. The 1:1 line relationships between the observed and estimated LAI, VWC, FB, DB and PH values were fitted and coefficient of determination (adj.  $R^2$ ), RMSE were computed. The lower value of obtained RMSE indicates a good predictive algorithm performance.

## 5.4 RESULTS AND DISCUSSION

The RFR, SVR, ANNR and LR algorithms applied in the present study were evaluated using adj.  $R^2$  and RMSE values. The variation of different winter wheat crop growth parameters at different growth stages are summarized in Table 5.2. The wheat crop growth parameters were found to increase more rapidly at early stages in comparison to the later growth stages of the crop. LAI, VWC and FB increased sharply after the tillering stage and then started decreasing after the heading stage of the wheat

crop. The DB and PH increased sharply till heading stage and then after found almost saturated.

**Table 5.2** Summary of the ground collected data for the winter wheat crop growth parameters

Crop growth parameters	08/01/15	08/02/15	25/02/15	05/03/15	21/03/15	10/04/15	29/04/15
LAI (m <sup>2</sup> /m <sup>2</sup> )	01.12	02.13	04.34	05.49	05.84	05.12	04.46
VWC (kg/m <sup>2</sup> )	01.89	03.85	06.78	09.33	09.90	08.24	05.37
FB (kg/m <sup>2</sup> )	02.84	06.35	11.37	15.54	16.37	14.74	11.88
DB (kg/m <sup>2</sup> )	00.95	02.50	04.59	06.22	06.47	06.50	06.51
PH (cm)	11.56	38.65	60.02	72.10	84.02	85.94	86.50

The scatter plots between observed and estimated values of LAI, VWC, FB, DB and PH were also compared to ensure the performances of the regression algorithms. Higher values of the adj. R<sup>2</sup> and lower values of RMSE correspond to better performance of an algorithm for the estimation of winter wheat growth parameters. Before evaluating the regression algorithms, the correlation analysis between  $\sigma^0$  and biophysical parameters was carried out using LR algorithm. The reasonable correlations were observed between computed  $\sigma^0$  vs. LAI (adj. R<sup>2</sup> = 0.75),  $\sigma^0$  vs. VWC (adj. R<sup>2</sup> = 0.84),  $\sigma^0$  vs. FB (adj. R<sup>2</sup> = 0.71),  $\sigma^0$  vs. DB (adj. R<sup>2</sup> = 0.65) and  $\sigma^0$  vs. PH (adj. R<sup>2</sup> = 0.63). RFR algorithm provided more accurate estimates of winter wheat growth parameters than the SVR, ANNR and LR algorithms. The results were also found good by SVR for LAI, VWC and by ANNR for the VWC of the wheat crop. Performance of RFR, SVR and ANNR algorithms were found good for the estimation of VWC because of its high sensitivity using VV-polarization at C-band. For the RFR performance, 224 initial trees were used to produce a graph showing average squared error rates against each tree for training and testing samples (Figures 5.3, 5.4, 5.5, 5.6 and 5.7). These graphs indicate an optimum number of trees 100 which showed the lowest error and a stable response.

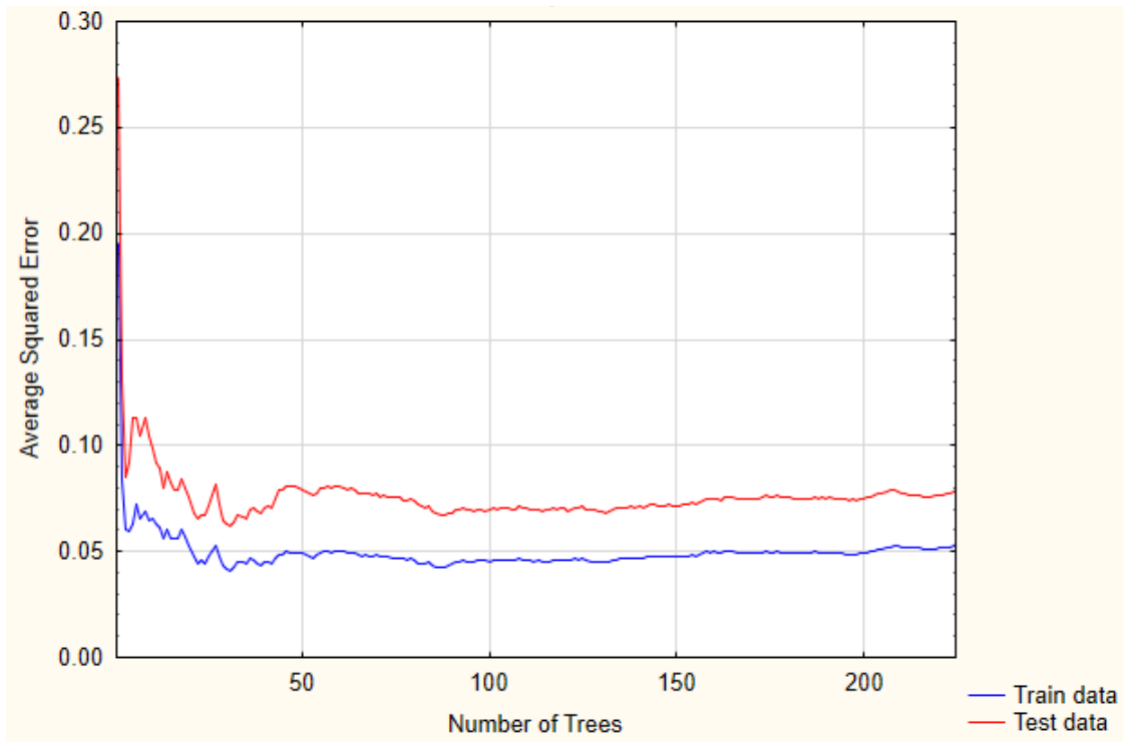


**Figure 5.3** Average square error rates against number of trees in training and testing data in the implementation of LAI estimation

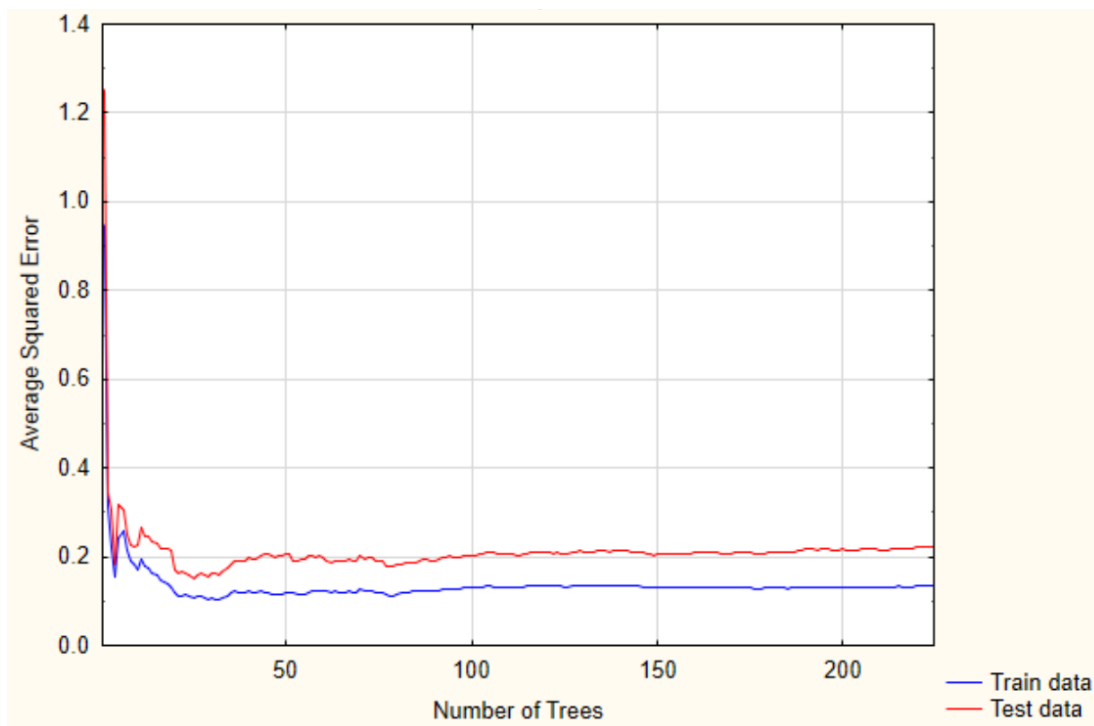


**Figure 5.4** Average square error rates against number of trees in training and testing data in the implementation of VWC estimation

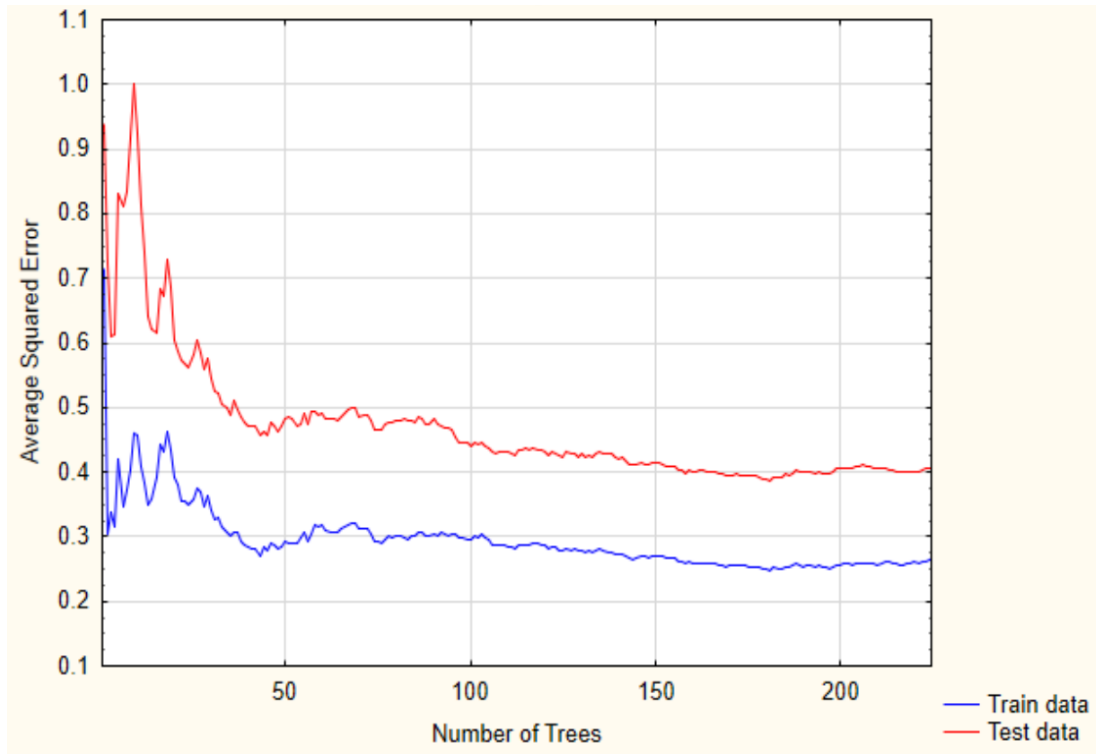


**Figure 5.5** Average square error rates against number of trees in training and testing data in the implementation of FB estimation

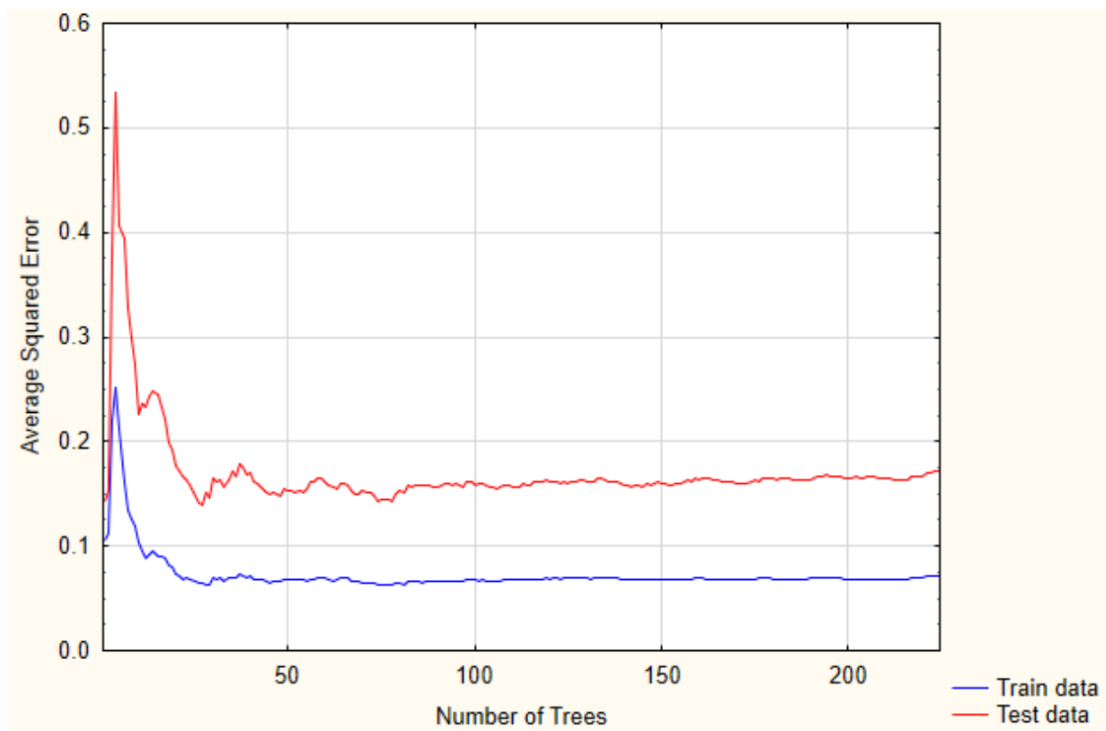


**Figure 5.6** Average square error rates against number of trees in training and testing data in the implementation of DB estimation

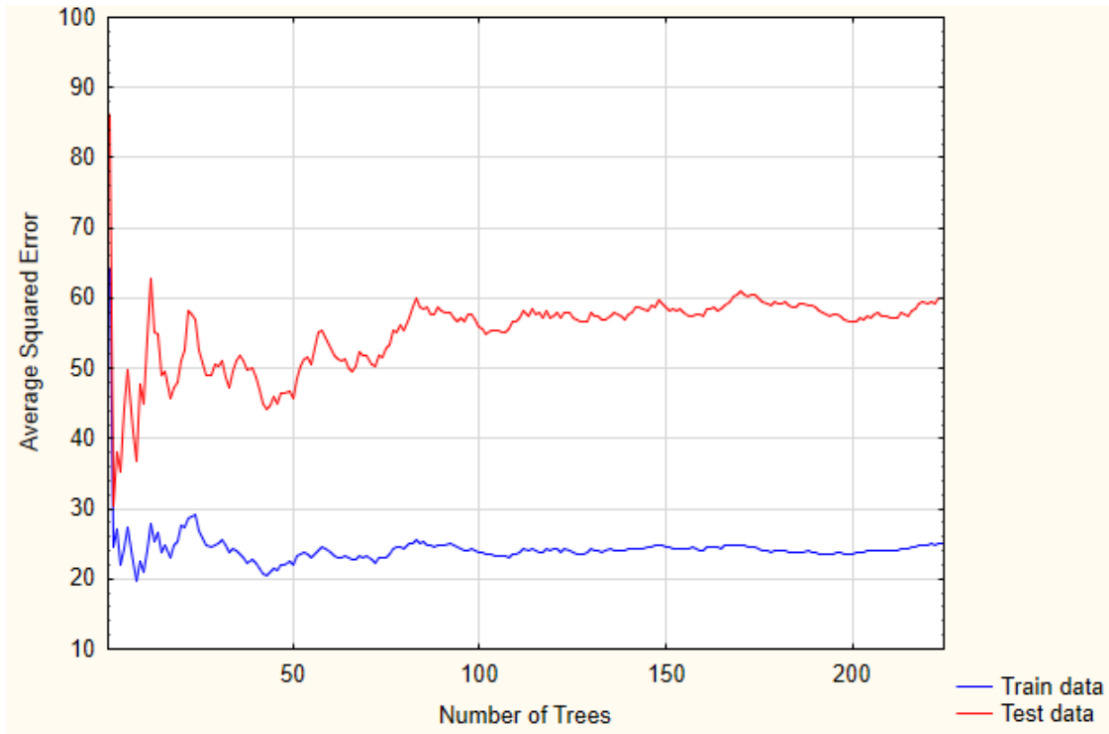


**Figure 5.7** Average square error rates against number of trees in training and testing data in the implementation of PH estimation

The overall high correlation was found between training and testing data for VWC while poor correlation showed for PH using RFR algorithm. Good correlations were also found between training and testing data-sets for LAI, FB and DB using RFR algorithm. The observed LAI covered a range between 1.12 to 5.84  $\text{m}^2\text{m}^{-2}$  for the wheat crop in the present study. RFR algorithm achieved higher value of adj.  $R^2$  (0.95) than SVR, ANNR and LR algorithms with adj.  $R^2$  (0.90, 0.86 and 0.76 respectively) values. The lesser value of RMSE (0.29) using RFR in comparison to SVR (0.46), ANNR (0.52) and LR (0.63) showed better estimation of LAI using RFR among all the algorithms. The RMSE for the LAI using RFR algorithm was also found lowest in comparison to all other crop parameters. The estimated values of winter wheat parameters were found closer to the 1:1 line using RFR algorithm. SVR algorithm showed overestimated values of LAI at booting and heading stages whereas the values estimated by ANNR were found overestimated at almost every growth stage except at

the ripening stage. The overestimated values of LAI were found at the tillering and booting stages. Whereas, underestimated values were found at the ripening stage using LR algorithm. Figure 5.8 shows the scatter plots of observed and estimated LAI values of winter wheat by RFR, SVR, ANNR and LR algorithms.

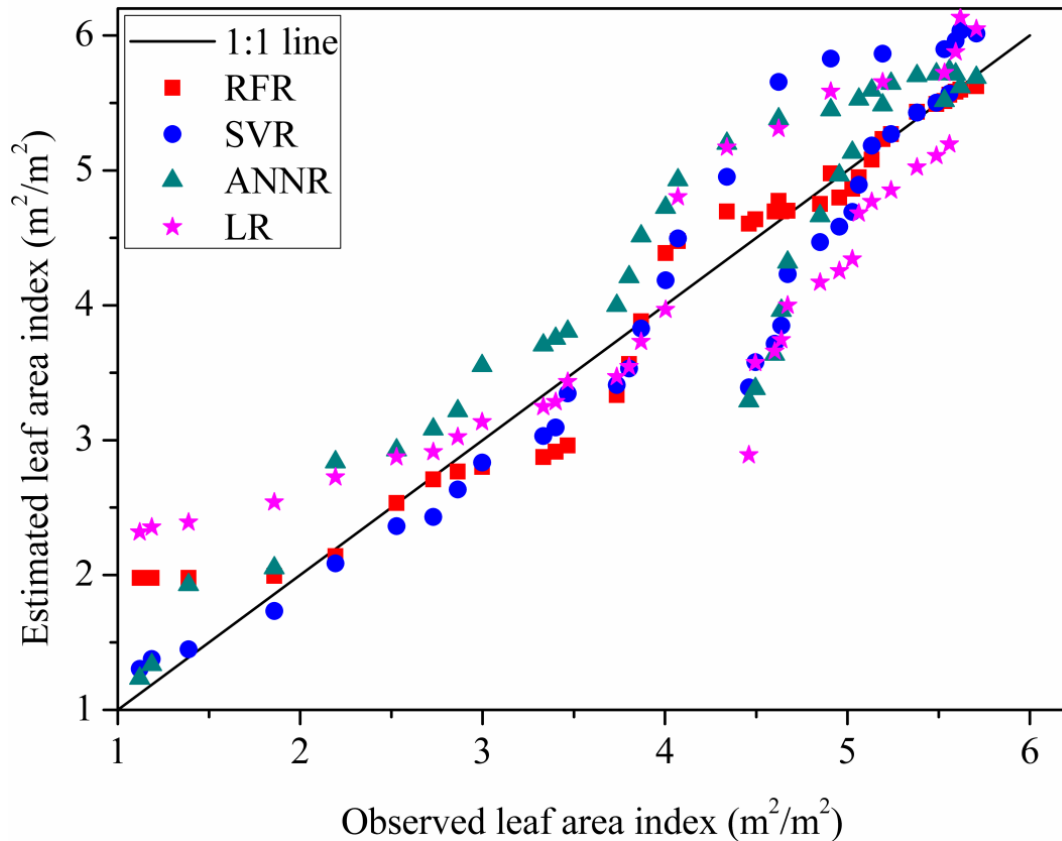


**Figure 5.8** Scatter plots of observed and estimated LAI values for winter wheat crop by RFR, SVR, ANNR and LR algorithms

The highest sensitivity showed for VWC using RFR (adj.  $R^2 = 0.96$ ; RMSE = 0.45), SVR (adj.  $R^2 = 0.93$ ; RMSE = 0.65), ANNR (adj.  $R^2 = 0.92$ ; RMSE = 0.72) and LR (adj.  $R^2 = 0.84$ ; RMSE = 0.84) algorithms in comparison to LAI, FB, DB and PH of winter wheat crop. The estimation of VWC was found better by all the algorithms using VV-polarization at C-band. The higher sensitivity of VWC found in comparison to FB of winter wheat at VV-polarization at C-band was also reported (Kim et al., 2014). Using RFR, observed offsets in LAI, VWC, FB, DB and PH estimation were negligible,

while SVR and ANNR clearly showed over estimation at booting and heading crop stages. The overestimated values of VWC were found at the tillering and booting stages for the LR algorithm. The estimated results by RFR algorithm for the VWC were close to the 1:1 line, which is an indicator of a robust and well-calibrated algorithm. Substantial increase in RFR algorithm robustness, less scattering and a better fit of the regression line was obtained for the accurate estimation of wheat parameters. The problem of under/overfitting was less detected in case of RFR algorithm. Figure 5.9 shows scatter plots of observed and estimated VWC values for winter wheat by using RFR, SVR, ANNR and LR algorithms.

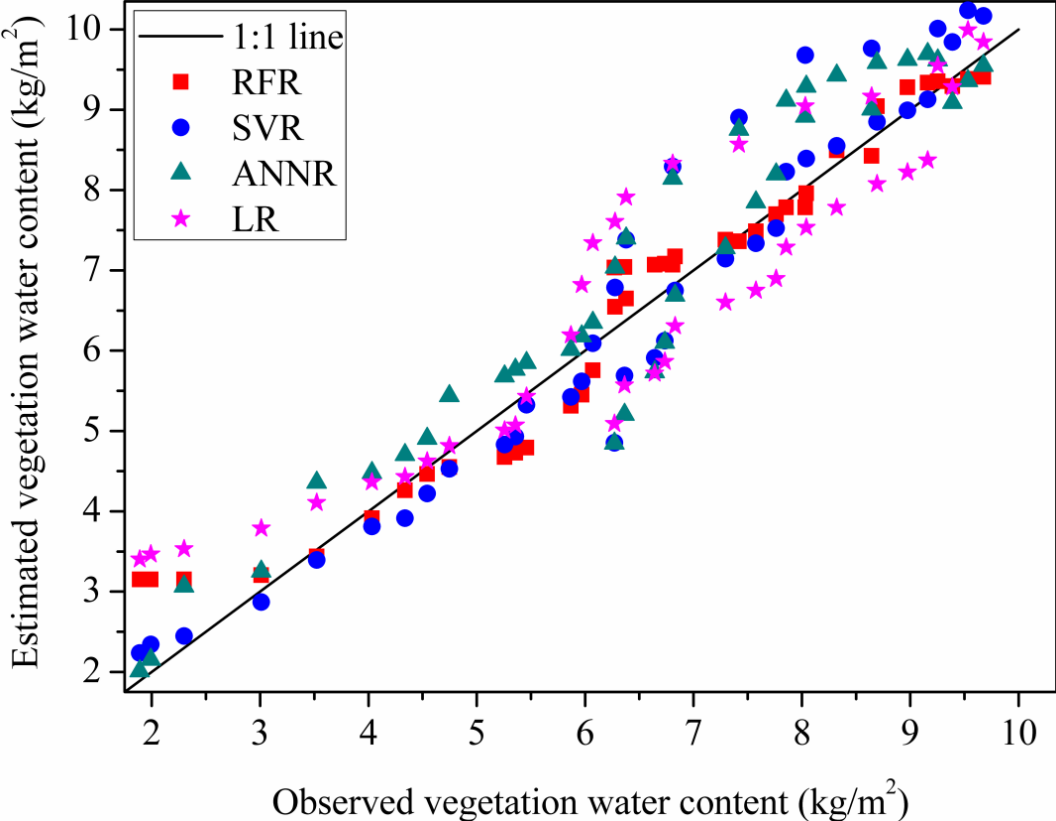


**Figure 5.9** Scatter plots of observed and estimated VWC values for winter wheat crop by RFR, SVR, ANNR and LR algorithms

The high values of adj.  $R^2 = 0.95$  and  $RMSE = 0.84$  were found for FB using RFR because the estimated values of FB were found almost close to 1:1 line. The results using SVR (adj.  $R^2 = 0.85$ ;  $RMSE = 1.47$ ) were also found good because at the early



stages, the estimated values of FB were found close to 1:1 line. At the later growth stages (booting and heading), the estimated values of FB were overestimated using SVR algorithm. High overestimated values were also found using ANNR algorithm at early as well as later stages. The overestimated values of FB at the tillering and booting, whereas, underestimated values of FB were found at ripening stages using LR algorithm. This fact indicates a more reliable algorithm performance of RFR in comparison with the SVR, ANNR and LR algorithms. The differences between RFR, SVR, ANNR and LR algorithms were also obvious in the scatter plots. Figure 5.10 shows the scatter plots of observed and estimated FB values for winter wheat based on RFR, SVR, ANNR and LR algorithms.

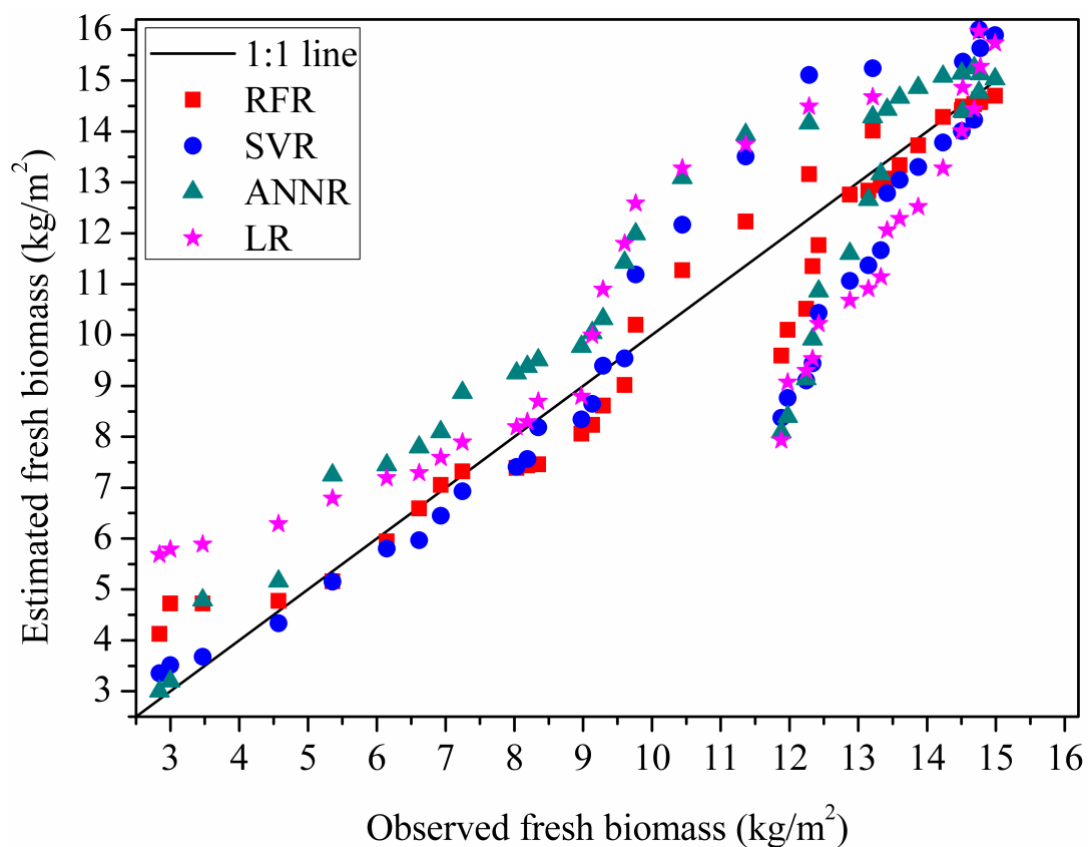


**Figure 5.10** Scatter plots of observed and estimated FB values for winter wheat crop by RFR, SVR, ANNR and LR algorithms

In the case of DB estimation, there was a large difference observed in the estimated values of DB by RFR (adj.  $R^2 = 0.93$ , RMSE = 0.43) in comparison to SVR

(adj.  $R^2 = 0.79$ , RMSE = 0.96), ANNR (adj.  $R^2 = 0.76$ , RMSE = 0.77) and LR (adj.  $R^2 = 0.68$ , RMSE = 0.90) algorithms. However, some overestimation was observed at booting and heading stages of the crop using RFR algorithm. Table 5.3 summarizes the results of the adj.  $R^2$  and RMSE using different regression algorithms.

**Table 5.3** Summary of the results in the adj.  $R^2$  and RMSE using RFR, SVR, ANNR and LR algorithms

Growth parameters	Algorithms	Regression equations	adj- R square	RMSE
LAI ( $m^2/m^2$ )	RFR	$y = 0.36+0.92x$	0.95	0.29
	SVR	$y = -0.21+1.04x$	0.90	0.46
	ANNR	$y = 0.52+0.92x$	0.86	0.52
	LR	$y = 1.00+0.76x$	0.76	0.63
VWC ( $kg/m^2$ )	RFR	$y = 0.49+0.94x$	0.96	0.45
	SVR	$y = -0.49+1.09x$	0.93	0.65
	ANNR	$y = 0.30+1.01x$	0.92	0.72
	LR	$y = 1.22+0.83x$	0.84	0.84
FB ( $kg/m^2$ )	RFR	$y = 0.62+0.92x$	0.95	0.84
	SVR	$y = 0.03+0.97x$	0.85	1.47
	ANNR	$y = 1.70+0.88x$	0.82	1.58
	LR	$y = 3.01+0.73x$	0.73	1.86
DB ( $kg/m^2$ )	RFR	$y = 0.57+0.88x$	0.93	0.43
	SVR	$y = 0.82+0.65x$	0.79	0.96
	ANNR	$y = 1.09+0.71x$	0.76	0.77
	LR	$y = 1.46+0.61x$	0.68	0.90
PH (cm)	RFR	$y = 8.49+0.85x$	0.90	7.74
	SVR	$y = 13.38+0.75x$	0.78	11.40
	ANNR	$y = 9.75+0.79x$	0.71	13.12
	LR	$y = 22.53+0.60x$	0.66	14.14

where x and y were the observed and estimated crop growth parameters, respectively.

Under estimation at later stages (heading and ripening) using SVR and overestimation (booting and heading)/underestimation (ripening) stages were observed using ANNR algorithm due to the large difference between observed and estimated values. The overestimated values of DB at tillering and booting stages, whereas underestimated values of DB at ripening stage were found using LR algorithm. Almost similar results were found using SVR and ANNR algorithms. Figure 5.11 shows the scatter plots of observed and estimated DB values for winter wheat by RFR, SVR, ANNR and LR algorithms.

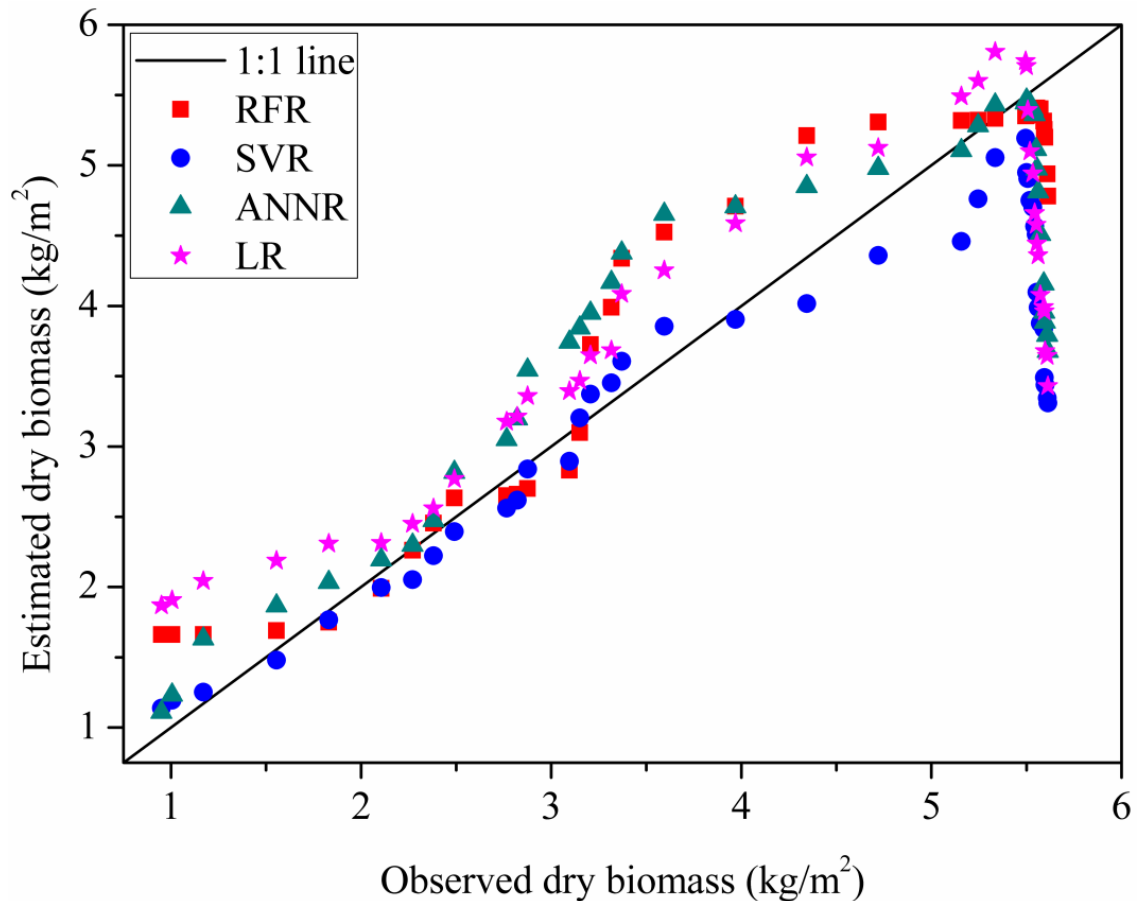


**Figure 5.11** Scatter plots of observed and estimated DB values for winter wheat crop by RFR, SVR, ANNR and LR algorithms

In the case of PH estimation, the estimated values of PH were found closer to 1:1 line at the early growth stages using RFR (adj.  $R^2 = 0.90$  and RMSE = 7.74) and SVR (adj.  $R^2 = 0.78$  and RMSE = 11.40) algorithms. These values were found over estimated at booting and heading, whereas, the underestimation were observed at the ripening stages. ANNR (adj.  $R^2 = 0.71$  and RMSE = 13.12) algorithm has shown more or less underestimated (tillering and jointing stages) values of PH at the early stages of the winter wheat crop while highly overestimated (booting and heading stages)/ underestimated (ripening) PH values were obtained at the later growth stages. The lowest adj.  $R^2$  (0.66) and highest RMSE (14.14) obtained by LR indicates its less sensitivity for the estimation of PH at VV polarization. The high overestimated values of PH at the tillering, booting and heading stages and underestimated values of PH at

the ripening stage were the major reasons for the poor results shown by the LR algorithm. Figure 5.12 illustrates the scatter plots of observed and corresponding estimated values of PH using RFR, SVR, ANNR and LR algorithms.

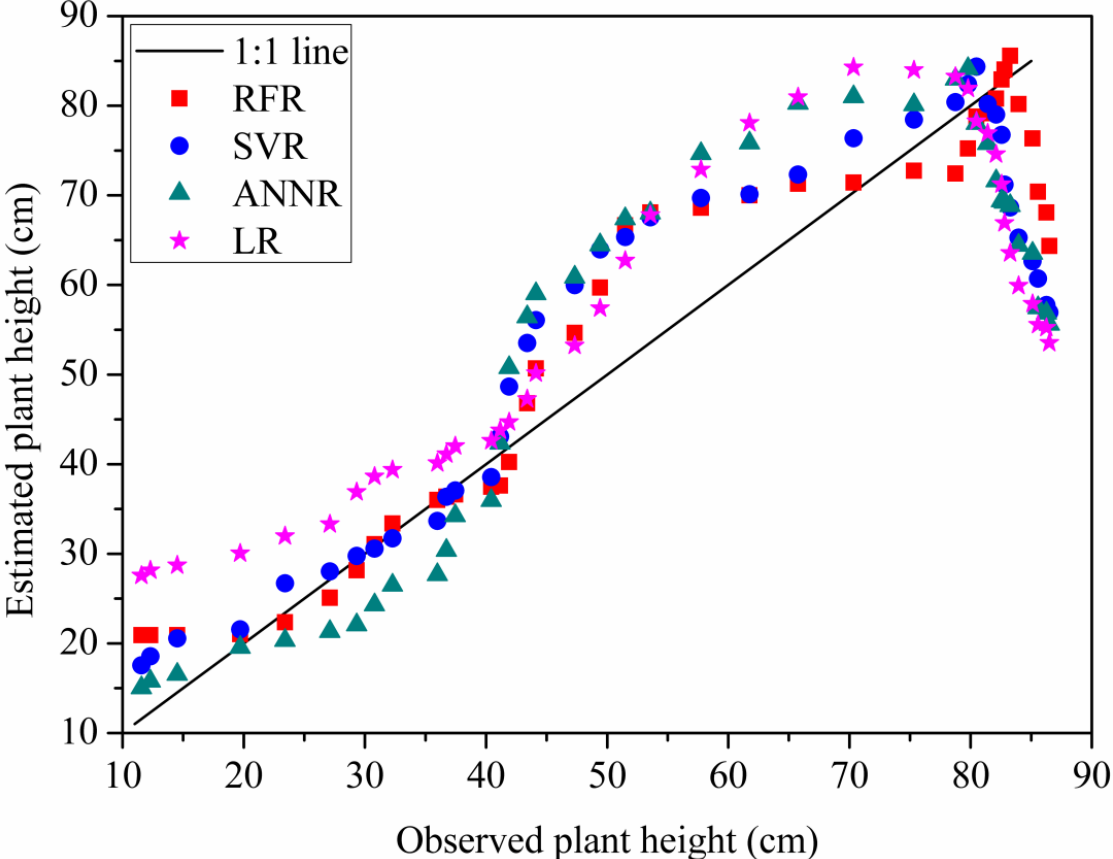


**Figure 5.12** Scatter plots of observed and estimated PH values for winter wheat crop by RFR, SVR, ANNR and LR algorithms

For the data-set used in the present study, the ANNR and LR algorithm showed under/over estimation for almost all the winter wheat parameters. LR provided better results, however, still showed inferior performance than RFR, SVR and ANNR algorithms. The under/over estimation of winter wheat parameters at the initial and later growth stages were problematic and this occurred in the scatter plots drawn between observed and estimated values by almost all the algorithms used. The random scattering occurred at the later growth stages was one of the reasons for getting the under/overestimated values of the crop growth parameters. ANNR algorithm was often

referred as a black-box algorithm that could encounter an over fitting problem on the test data-set (Qiu and Jensen, 2004).

RFR algorithm provided high values of adj.  $R^2$  for LAI, VWC, FB, DB and PH in comparison to SVR, ANNR and LR algorithms. Nevertheless, the values of adj.  $R^2$  (0.93) obtained by SVR were found close to RFR (0.96) and ANNR (0.92) for the estimation of VWC. The values of adj.  $R^2$  for LAI, FB, DB and PH using SVR were found slightly higher than the ANNR algorithm. Poor performance shown by ANNR may be due to non-availability of large amounts of sampling data. However, the performance of RFR and SVR were found good even for small amounts of sampling data used. The learning ability of ANNR was too strong during training, thus the algorithm cannot reflect the hidden rules of the samples and weaken the prediction ability of the algorithm (Wang et al., 2016).

## **5.5 CONCLUSION**

The present study demonstrated a successful application of C-band Sentinel-1A SAR images for the estimation of winter wheat crop growth parameters using RFR, SVR, ANNR and LR algorithms. RFR algorithm achieved relatively more accurate results in comparison to SVR, ANNR and LR algorithms. The investigation demonstrates the excellent capability of the Sentinel-1A SAR data at C-band for the monitoring of agricultural areas. RFR model provides a useful exploratory and predictive tool for estimating winter wheat crop growth parameters. The results of the present study may provide the valuable information for the satellites to be launched in the near future for the accurate and timely monitoring of different crops.